Available online at www.sciencedirect.com

ScienceDirect

Procedia CIRP 58 (2017) 263 – 268

www.elsevier.com/locate/procedia

16th CIRP Conference on Modelling of Machining Operations

An analytical method for prediction of material deformation behavior in grinding using single grit analogy

Dinesh Setti*[a], Benjamin Kirsch[a], J.C. Aurich[a]

[a]*Institute for Manufacturing Technology and Production Systems, University of Kaiserslautern, Gottlieb-Daimler-Str., 67663, Kaiserslautern, Germany*

*Corresponding author. Tel.: 49-631-205-3473; fax: +49-631-205-3238. E-mail address: dinesh.setti@mv.uni-kl.de

Abstract

FEM simulation and single grit experimental techniques are available to get an insight into the chip formation mechanism in grinding operations. However, those are case specific. In the present work, an analytical method has been developed by considering specific energy criteria and Johnson's indentation theory to predict the modes of chip formation. The force acting on an abrasive grit at every instance in a trajectory path has been calculated by considering grit size, wheel size, kinematic conditions and work material properties. Yield coefficient and non-dimensional strain at the grit-work interaction have been computed to identify mainly the ploughing to cutting transition phase.

Peer-review under responsibility of the scientific committee of The 16th CIRP Conference on Modelling of Machining Operations

Keywords: Single grit; grinding; cutting; indentation; grit cutting depth; minimum chip thickness; micro milling; modelling;

1. Introduction

In a grinding operation, abrasive grits on the wheel surface move over the workpiece surface in a trajectory path and remove the material in the form of chips. In this process of grit penetration into the workpiece surface, normal and tangential forces are generated between the wheel and work interface. Along the path of a grit, the grit penetration depth increases in the contact zone. As a consequence, the workpiece material is subjected to three different modes. These are rubbing, ploughing, and cutting [1] as shown in Fig. 1. In the rubbing phase, abrasive grits rub over the surface and cause elastic deformation to the work surface. In the ploughing phase, the grit penetrates and ploughs the surface causing ridges without material removal. In the last phase, the grit penetrates deeply into the workpiece surface and forms a chip.

In a grinding process, some abrasive grits on the wheel surface may experience only the rubbing phase, most of the grits may experience both rubbing and ploughing phase, and very few grits may experience all the three phases. The transition from one phase to another phase depends on the penetrated depth value. In the first phase, contact between grit and work material causes elastic material deformation only.

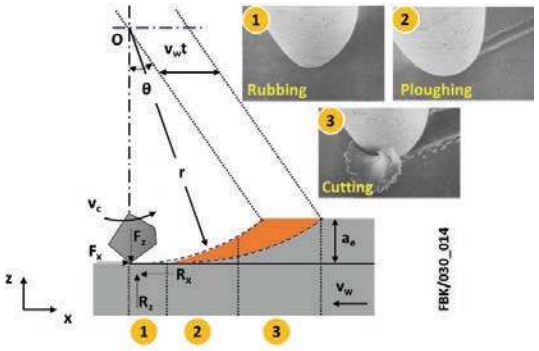

Fig. 1. Three different phases of material deformation modes in single grit trajectory path (SEM images from Hokkirigawa and Kato [2])

The increase of penetration depth results in an additional plastic deformation, where the second phase begins. When the penetration depth reaches a specific value, chip removal takes place. Phase III hence can be called the cutting phase. This specific penetration depth value is also known as 'grit cutting

Peer-review under responsibility of the scientific committee of The 16th CIRP Conference on Modelling of Machining Operations
doi:10.1016/j.procir.2017.03.193

Nomenclature

a	projected radius of the deformed contact
a_e	given depth of cut
b	half of the grit cutting width
BHN	brinell hardness number
d_g	diameter of abrasive grit
D	diameter of grinding wheel
E	equivalent elastic modulus
E_1	elastic modulus of grit material
E_2	elastic modulus of workpiece material
f	interface friction ratio (shear stress to flow stress ratio)
F	total grinding force = $\sqrt{F_x^2 + F_z^2}$
$F_{brinell}$	brinell indentation force
$F_{cut,g}$	cutting force acting on abrasive grit
$F_{n,cut,g}$	normal force acting on single grit in cutting phase
$F_{n,g}$	normal force component acting on single grit
$F_{n,plou,g}$	normal force on single grit in ploughing phase
$F_{n,rub,g}$	normal force acting on single grit in rubbing phase
$F_{plou,g}$	ploughing force acting on abrasive grit
$F_{rub,g}$	rubbing force acting on abrasive grit
$F_{t,cut,g}$	tangential force acting on grit in cutting phase
$F_{t,\,g}$	tangential force acting on single abrasive grit
$F_{t,\,plou,g}$	tangential force on single grit in ploughing phase
$F_{t,rub,g}$	tangential force on single grit in rubbing phase
F_x	total horizontal force component
F_z	total vertical force component
h'	minimum chip thickness
h_m	maximum uncut chip thickness
m	mass of abrasive grit
p_m	mean contact pressure
r	radius of grinding wheel
r_g	radius of the abrasive grit
R_e	grit cutting edge radius
R_x	horizontal resistance component
R_z	vertical resistance component
v_c	velocity of the grinding wheel
v_w	velocity of the workpiece
$\ddot{x}$	horizontal acceleration of abrasive grit
Y	tensile yield strength of the workpiece material
$\ddot{z}$	vertical acceleration of abrasive grit
τ_s	shear strength of workpiece
λ	effective grit angle
γ	rake angle
α	grit attack angle (90°+γ)
β	friction angle
$\emptyset$	shear angle
θ	rotation angle of the wheel
μ_{rub}	coefficient of friction during rubbing phase
μ_{plou}	coefficient of friction during ploughing phase
μ_{cut}	coefficient of friction during cutting phase
ϑ_1	poisson's ratio of grit material
ϑ_2	poisson's ratio of workpiece material

depth' [3] or 'critical depth of cut' [4] or 'Plastic transition'[5]. The 'critical depth of cut' also refers to the transition from brittle to ductile material removal when grinding brittle materials[6]. The 'Plastic transition' can be misinterpreted as the transition from Phase I to Phase II. Hence, in this paper the transition from Phase II to Phase III will be denoted as the grit cutting depth. Corresponding uncut chip thickness value related to critical depth of cut is denoted as minimum chip thickness as shown in Fig. 2. As underlying material removal mechanism in grinding is similar to micro machining, grit cutting depth can be termed as minimum chip thickness in micro machining processes.

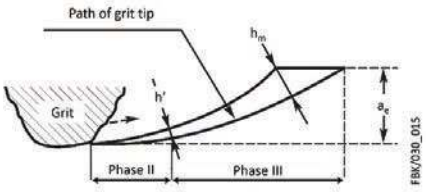

Fig. 2. Illustration of phase II followed by transition to phase III in grinding zone

In a grinding process, for a given depth of cut, obtainable maximum uncut chip thickness value for a single grit can be predicted using the following equation [7].

$$h_m = 2\pi D \left(\frac{v_w}{v_c}\right)\sqrt{\frac{a_e}{D}} \quad (1)$$

For the same depth of cut value, it is possible to have different chip thickness values depending upon wheel speed, workpiece speed and wheel diameter. Depending upon these kinematic conditions critical depth of cut value also differs. Uncut chip thickness is the only parameter, which can take care of different kinematic conditions. Hence, in the present work, all the results are explained in terms of uncut chip thickness and minimum chip thickness.

Advanced simulation and experimental techniques are available to give an insight into the chip formation mechanism in machining operations. In the case of grinding, such studies on material removal mechanism are difficult due to several factors. Besides high cutting speeds and rate of deformation, modeling of the grinding wheels themselves is a challenge. The grits are randomly distributed on the wheel surface and are of undefined or unknown geometry and shape. However, the knowledge about the grit cutting depth is essential for understanding and optimizing the grinding process. In grinding, the sequential motion of individual grits and depth of cut at micron level leads to a macroscopic material removal. As a result, the grinding performance can only be described by individual grit's cutting behaviour.

To study the chip formation mechanism in grinding several analytical and numerical models were developed. In 1979, Challen and Oxley [8] presented different modes of material deformation such as rubbing, wear and cutting based on slip-line field theory when two conical asperities move on each other. Later the same slip-line field methodology was applied for grinding and polishing operations by considering the lubrication effect [9]. Lortz [10] presented a plane chip formation model based on the theory of slip-line fields in grinding by considering the kinematic conditions and the grit

shape as a sphere. Later Childs [11] extended this approach to wedge shapes also. Apart from the slip-line field method, there are several Finite Element modeling approaches considering idealized grit shapes [12, 13]. However, simulation time and obtaining suitable material models are limitations to these methods. There are several techniques like the quick-stop device method, single grit scratch method and indentation methods to study the chip formation mechanism experimentally. Out of these, the single grit scratch method is the most widely used. Early research on single grit grinding tests was performed by Takenaka [14]. He observed cutting action at extremely small depth of cuts (<0.4 μm) and also reported the three phases of material removal: rubbing, ploughing and chip formation. Doyle [15] investigated the chip formation of abrasive grits having large negative rake angles using the quick-stop method. Aurich and Steffes [16] observed the effect of cutting edge angle on chip formation using single grit experiments. Barge et al. [17] observed a decreasing amount of plastic deformation with increasing cutting speeds. From the above literature, it can be observed that several researchers have made an attempt to study the cutting mechanism in grinding by physical models, FEM simulations, and also by conducting experiments. Chip formation modes have been investigated mostly by experimental techniques only, which are case specific and highly depend on grit size and shape. In this situation, an analytical model could facilitate the prediction of minimum chip thickness values irrespective of kinematic conditions and work materials. Hence, in the present work an analytical method has been developed by considering Johnson's indentation theory and specific energy variation with material removal rate to predict the minimum chip thickness value.

2. Analytical method

The method developed in the present investigation should be regarded as a first approximation by considering the grinding wheel size, grit size, kinematic conditions and work material properties to determine the minimum chip thickness value. The shape of abrasive grits is assumed as spherical. Although this is a simplistic assumption, it is still used because of its analytical convenience. For the proposed method different shapes of grits can later also be implemented.

Grit trajectory path and corresponding equation of motion

Fig. 1 shows the trajectory path of a single grit relative to the workpiece for the kinematic analysis. A global coordinate system is set with its origin 'O', which is fixed at the center of the wheel.

The trajectory path of a grit as a function of 'θ' in x and z directions can be expressed as

$$x(\theta) = r\sin\theta \pm r\left(\frac{v_w}{v_c}\right)\theta \tag{2}$$

$$z(\theta) = r - r\cos\theta \tag{3}$$

where x and z are the coordinates of the abrasive grit. The plus sign in equation 2 refers to up-grinding as shown in figure 2, and the negative sign refers to down-grinding process.

The value of θ corresponding to given depth of cut can find out using the following equation.

$$\theta = sin^{-1}\left(\frac{\sqrt{r^2-(r-a_e)^2}}{r}\right) \tag{4}$$

In equation 3, the value of z with respect to angle θ gives the instantaneous depth of cut value. i.e. at the beginning of cut $\theta = 0^o$ and $z = 0$, and at the end of cut $\theta = \theta_{max}$ and $z = a_e$. Substitution of z values for a_e in equation 1 gives the uncut chip thickness (h) values.

If we consider the trajectory path of the grit into workpiece as the penetration process, according to Newton's second law of motion, the total forces acting on the grit in horizontal and vertical directions can be described with the help of equation of the motion of the grit as given below [18, 19]

$$F_x - R_x = m\ddot{x} \tag{5}$$

$$F_z - R_z = m\ddot{z} \tag{6}$$

The resistance force acting on abrasive grit in horizontal and vertical directions is equal to the tangential and normal grinding force components. The tangential and normal grinding force components can be predicted based on the available models as explained in section 2.2. As explained in section 1, material deformation modes in grinding consists of elastic, elastic-plastic and plastic deformation phases and these phases have been modeled with the help of Hertzian contact theory for elastic surfaces, Brinell indentation model and Merchant's metal cutting model respectively.

2.1. Force prediction

The grinding force acting on abrasive grit consists of three force components: rubbing, ploughing, and cutting[20].

$$F = F_{rub,g} + F_{plou,g} + F_{cut,g} \tag{7}$$

$$F_{n,g} = F_{n,rub,g} + F_{n,plou,g} + F_{n,cut,g} \tag{8}$$

$$F_{t,g} = F_{t,rub,g} + F_{t,plou,g} + F_{t,cut,g} \tag{9}$$

Normal rubbing force component of the grit can be calculated using Hertzian contact theory as given below[21].

$$F_{n,rub,g} = \frac{4}{3}E\, r_g^{1/2} h_m^{\ 3/2} \tag{10}$$

$$\frac{1}{E} = \frac{(1-\vartheta_1^2)}{E_1} + \frac{(1-\vartheta_2^2)}{E_2} \tag{11}$$

Further, the tangential rubbing force component can be calculated as

$$F_{t,rub,g} = \mu_{rub} F_{n,rub,g} \tag{12}$$

Coefficient of friction during rubbing phase is given by [8]

$$\mu_{rub} = \frac{A\,\sin\alpha + \cos(\cos^{-1} f - \alpha)}{A\,\cos\alpha + \sin(\cos^{-1} f - \alpha)} \tag{13}$$

where $A = 1 + \frac{\pi}{2} + cos^{-1} f - 2\alpha - 2\,sin^{-1}\frac{sin\,\alpha}{(1-f)^{1/2}}$

For a spherical grit of radius r_g, attack angle (α) and rake angle (γ) can be calculated using the equation 14 and 15.

$$\alpha = \sin^{-1}\left(\frac{b}{r_g}\right) \tag{14}$$

$$\gamma = \sin^{-1}\left(\frac{r_g - h_m}{r_g}\right) \quad (15)$$

where $b = \sqrt{r_g^2 - (r_g - h_m)^2}$

The normal and tangential force for ploughing component can be expressed similar to Brinells hardness test. It is given by [22]

$$F_{n,plou,g} = F_{brinell}(\cos\lambda - \mu_{plou}\sin\lambda) \quad (16)$$

$$F_{t,plou,g} = F_{brinell}(\sin\lambda + \mu_{plou}\cos\lambda) \quad (17)$$

where

$$F_{brinell} = 15.4(BHN)(d_g)(d_g - \sqrt{d_g^2 - d_g^2\sin^2\lambda}),\ \lambda = \cos^{-1}\left(1 - \frac{h_m}{r_g}\right)$$

coefficient of friction during ploughing phase is given by [8]

$$\mu_{plou} = \frac{\{1 - 2\sin\beta + (1-f)^{1/2}\}\sin\alpha + f\cos\alpha}{\{1 - 2\sin\beta + (1-f)^{1/2}\}\cos\alpha - f\sin\alpha} \quad (18)$$

where $\beta = \alpha - \frac{\pi}{4} - \frac{1}{2}\cos^{-1} f + \sin^{-1}\frac{\sin\alpha}{(1-f)^{1/2}}$

As stated by Wang et al. tangential cutting force component for single grit can be expressed as [23]

$$F_{t,cut,g} = \int_{\frac{\pi}{2}}^{\gamma} \frac{\tau_s \cos(\beta - \gamma)}{\sin\emptyset\cos(\emptyset + \beta - \gamma)} 2r_g^2\cos^2\gamma\, d\gamma \quad (19)$$

$$F_{n,cut,g} = F_{t,cut,g}/\mu_{cut} \quad (20)$$

where $\emptyset = \frac{\pi}{4} - \frac{\beta}{2} + \frac{\gamma}{2}$ *(Ernst and Merchant criteria),*

$\beta = \tan^{-1}\mu_{cut}$, and $\mu_{cut} = \tan(\alpha - \frac{\pi}{4} + \frac{1}{2}\cos^{-1} f)$

Finally, by considering the equations 10, 12, 16, 17, 19, and 20 the normal force and tangential force acting on a single abrasive grit at each instance of trajectory path can be predicted using the equations 8 and 9.

2.2. Utilization of Johnson's indentation theory

Based on the total force acting on a single grit, further analysis can be done using Johnson's indentation theory[24]. Johnson has shown that the indentation of a hard indenter proceeds through several deformation regimes such as elastic, elastic-plastic, and fully plastic zones, which are similar to the deformation modes in grinding such as rubbing, ploughing, and cutting. These regimes are identified based on the following criteria [25].

If $p_m \leq 1.1Y$ (Elastic deformation)

If $1.1Y < p_m < 2.97Y$ (Elastic-plastic deformation)

If $p_m \geq 2.97Y$ (Fully plastic deformation)

From the obtained total force value, yield coefficient and non-dimensional strain values can be calculated using the following expressions [24]

$$\text{Yield coefficient } \left(\frac{p_m}{Y}\right) = \frac{2}{3}\left\{1 + \ln\left(\frac{Ea}{3Yr_g}\right)\right\} \quad (21)$$

$$\text{Non-dimensional strain} = \frac{Ea}{Yr_g} \quad (22)$$

Projected radius of the deformed contact can be calculated as

$$a = \frac{3Fr_g}{4E} \quad (23)$$

In a grinding process, the specific energy consumption varies from phase to phase. i.e. specific energy requirement is maximum in rubbing phase and minimum in cutting phase. Hence, from the variation in specific energy values also different deformation modes in grinding can be derived.

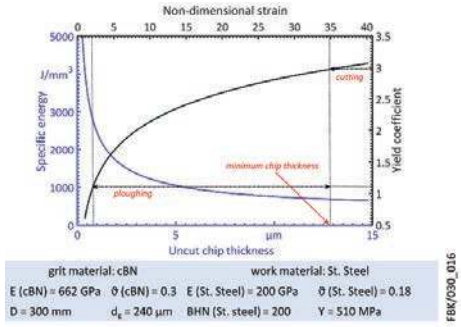

Fig. 3. Identification of minimum chip thickness based on non-dimensional stain and yield coefficient curve

Hence, in the present work, based on the cumulative analysis of specific energy variation with uncut chip thickness, and mean pressure variation with non-dimensional strain (i.e. where the mean pressure value reaches a value of 2.97 times the yield strength of work material and the corresponding uncut chip thickness value termed as minimum chip thickness), minimum chip thickness value has been identified in terms of uncut chip thickness as shown in Fig. 3.

3. Validation

In this section, the proposed method will be applied to different boundary conditions. If the variation in observed results is according to common knowledge, then it can be said that the method is qualitatively applicable. The quantitative accuracy will be evaluated in future works based on experimental data.

3.1. Influence of process parameters and material conditions on minimum chip thickness and deformation modes

The main aim of the present work is the prediction of different deformation modes in grinding as a function of kinematic conditions such as cutting speed, feed rate, wheel size, abrasive grit size and material properties. Hence, as a first step to validate the method, % of material deformation modes for different conditions have been predicted as shown in figure 6. Here, phase I (rubbing) + phase II (ploughing), and phase III (cutting) % of deformation modes have been predicted using the equations 24 and 25. It has been assumed that the thickness of the uncut chip increases linearly along its contact length.

$$\%\ of\ (phase\ I + phase\ II) = \left(\frac{h'}{h_m}\right)^2 \times 100 \quad (24)$$

$$\%\ of\ phase\ III = 100 - (\%\ of\ phase\ I\ \&\ II) \quad (25)$$

Further, as given by Shaw[26], for an unworn abrasive grit, the relation between the grit diameter and cutting edge radius can be considered as given below.

$R_e = 0.23 d_g$ (26)

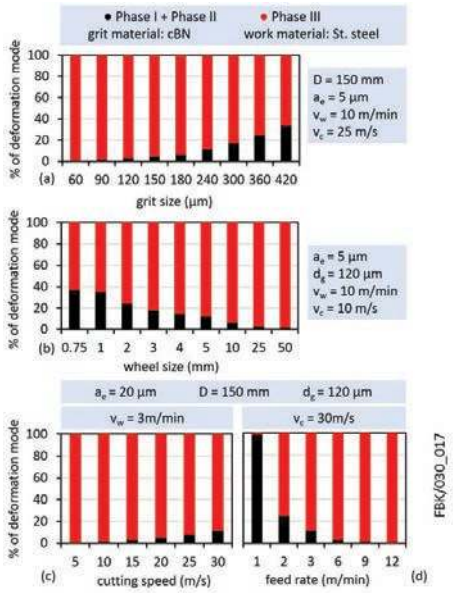

Fig. 4. Variation in material deformation mode with grit size, wheel size, cutting speed, and feed rate with a single grit

From the Fig. 4(a), it can be observed that, as the size of grit increases, more ploughing and rubbing action occurs due to an increase in the cutting edge radius value. Earlier, Hokkirigawa and Kato [2] also have made the similar kind of observation in terms of degree of penetration (ratio between the depth of penetration to cutting edge radius). The higher the value of the degree of penetration, the more cutting. In other words, grit negative rake angle increases with increasing grit diameter, resulting into a blunt grit. For efficient cutting, we need small negative rake angles, which is possible with small grits at large penetration depths.

According to Park and Liang [27], as the size of the wheel decreases, ploughing effect plays a more important role than the other two mechanisms. The results shown in Fig. 4(b) are also in line with this statement. Feed per cutting grit value decreases with increasing cutting speed and decreasing feed rate. Due to this, uncut chip thickness value would be less than the minimum chip thickness value, which promotes the ploughing and rubbing actions rather than the cutting. This variation can be seen in Fig. 4(c) and 4(d).

Fig. 5 shows the estimated minimum chip thickness values variation with grit size for different grit and work materials. It can be observed that the minimum chip thickness values have a linear relationship with grit cutting edge radius and varies significantly with the work material. It can be observed that difficult to machine materials like Ti-6Al-4V and Inconel 718 have higher minimum chip thickness values than other material like mild steel due to their elastic deflection nature and higher yield strength values. It can be observed that the nature of grit material also has an influence on the minimum chip thickness value as reported by Yuan et al. [28]

The minimum chip thickness to cutting edge radius ratio values were plotted against the E/Y ratio as shown in Fig. 6. The relationship between these can be expressed as an exponential function as given in equation 27.

$$\frac{h'}{R_e} = 0.7304 e^{-0.004\left(\frac{E}{Y}\right)} \quad (27)$$

Here both E and Y should have the same units i.e. either in MPa or GPa. The above specified relation holds good only for E/Y values in between 100-400.

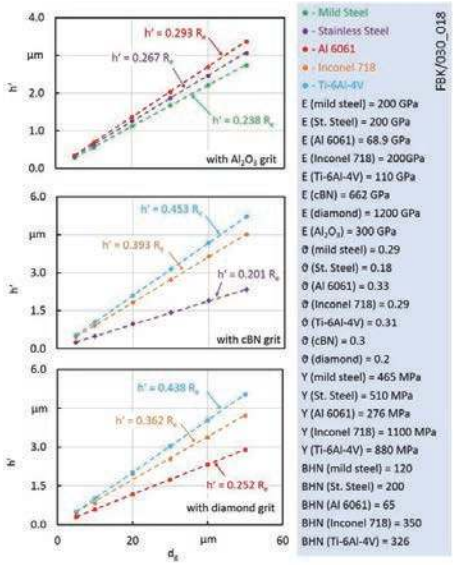

Fig. 5. Variation of minimum chip thickness values with different grit sizes, grit materials and work material combinations

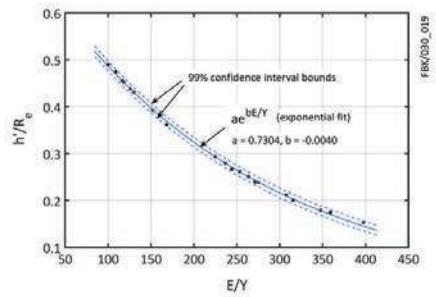

Fig. 6. Minimum chip thickness to cutting edge radius ratio variation with E/Y ratio

3.2. Comparison with the micro milling literature data

The milling analogy was utilized by several researchers in the past to analyze the grinding. The milling analogy is the starting point for the kinematic analysis and to characterize the material removal in grinding process. Hence the present methodology has been applied to available micro milling results to check the applicability.

From the comparisons shown in table 1, it can be said that the proposed method is showing the variation in minimum chip thickness (h′) values according to work material variations. It

can also be observed that the predicted values are in line with the available literature data.

Table 1: Comparison of the minimum uncut chip thickness to cutting edge radius ratio among different authors and workpiece materials (tool: Tungsten carbide, E_1 = 450 GPa, ϑ_1 = 0.22)

Ref.	Workpiece	E_2 (GPa)	ϑ_2	Y (MPa)	h'/R_e	Present method h'/R_e
[29] [32]	AISI 1045	200	0.29	530	0.22-0.36 0.29	0.24
[30]	AISI 1040	200	0.29	490	0.20-0.35	0.22
[30]	6082-T6 Aluminium	70	0.33	270	0.35-0.40	0.27
[31]	6061 Aluminium	69	0.33	276	0.23	0.28
[33]	AISI 4340	210	0.29	500	0.26	0.21
[34]	Aluminium	68.3	0.34	240	0.20-0.40	0.24
[35]	360 Brass	97	0.31	310	0.30	0.24

4. Conclusions

A method to predict the minimum chip thickness value for grinding has been developed. The method is based on Johnson's indentation theory and specific energy variation. The proposed method predicts the variations in material deformation modes with respect to various kinematic conditions such as cutting speed and feed rate, the size of the wheel, the size of the abrasive grits and material properties of wheel and workpiece materials. The predicted total grinding force value was fed back into the Johnson method to calculate yield coefficient and non-dimensional strain values. All the responses (specific energy, uncut chip thickness, non-dimensional strain and yield coefficient) were plotted together and from the mean pressure variation with yield strength, minimum chip thickness value was identified. Further predicted minimum chip thickness values had been verified with the available micro milling literature values. In future works, single grit experiments will be conducted to validate the approach.

Acknowledgement

The research presented in this paper was funded by the Deutsche Forschungsgemeinschaft DFG within the International Research Training Group IRTG 2057 "Physical Modeling for Virtual Manufacturing Systems and Processes".

References

[1] Hahn RS. On the nature of the grinding process, in: Proceeding of the 3rd MTDR Conference; 1962. p. 129-154.
[2] Hokkirigawa K, Kato K. An experimental and theoretical investigation of ploughing, cutting and wedge formation during abrasive wear. Tribol Int 1988;21:51-57.
[3] Rasim M, Mattfeld P, Klocke F. Analysis of the grain shape influence on the chip formation in grinding. J Mater Process Tech 2015;226:60-68.
[4] Öpöz TT, Chen X. Experimental study on single grit grinding of Inconel 718. P I Mech Eng B-J Eng 2015;229:713-726.
[5] Anderson D, Warkentin A, Bauer R. Experimental and numerical investigations of single abrasive-grain cutting. Int J Mach Tool Manu 2011;51:898-910.
[6] Bifano TG, Dow TA, Scattergood RA. Ductile-regime grinding of brittle materials: Experimental results and the development of a model. In: Arnold JB, Parks RE, editors. Advances in fabrication and metrology for optics and large optics. 1989. p. 108-115.
[7] Werner G. Kinematik und Mechanik des Schleifprozesses. PhD thesis. RWTH Aachen University;1971.
[8] Challen JM, Oxley PLB. An explanation of the different regimes of friction and wear using asperity deformation models. Wear 1979;53:229-243.
[9] Challen JM, Oxley PLB. Slip-line fields for explaining the mechanics of polishing and related processes. Int J Mech Sci 1984;26:403-418.
[10] Lortz W. A model of the cutting mechanism in grinding.Wear 1979;53:115-128.
[11] Childs T. The mapping of metallic sliding wear. P I Mech Eng C-J Mec 1988;202:379-395.
[12] Öpöz TT, Chen X. Single grit grinding simulation by using finite element analysis. AIP Conf Proc 2011;1315:1467-1472.
[13] Holtermann R, Menzel A, Schumann S, Biermann D, Siebrecht T, Kersting P. Modelling and simulation of internal traverse grinding: Bridging meso- and macro-scale simulations. Prod Engineer 2015;9:451-463.
[14] Takenaka N. A study on the grinding action by single grit. CIRP Ann Manuf Techn1966;13:183-190.
[15] Doyle ED. On the formation of a quick-stop chip during single grit grinding. Wear 1973;24:249-253.
[16] Aurich JC, Steffes M. Single grain scratch tests to determine elastic and plastic material behavior in grinding. Adv abrasive technol 2011;325:48-53.
[17] Barge M, Rech J, Hamdi H, Bergheau JM. Experimental study of abrasive process. Wear 2008;264:382-388.
[18] Hashish M. A modeling study of metal cutting with abrasive waterjets. J Eng Mater-T ASME 1984;106:88-100.
[19] Finnie I, McFadden DH. On the velocity dependence of the erosion of ductile metals by solid particles at low angles of incidence. Wear 1978;48:181-190.
[20] Durgumahanti USP, Singh V, Rao PV. A new model for grinding force prediction and analysis. Int J Mach Tool Manu 2010;50:231-240.
[21] Xie Y, Williams JA. The prediction of friction and wear when a soft surface slides against a harder rough surface. Wear 1996;196:21-34.
[22] Hecker RL, Liang SY, Wu XJ, Xia P, Jin DGW. Grinding force and power modeling based on chip thickness analysis. Int J Adv Manuf Tech 2007;33:449-459.
[23] Wang D, Ge P, Bi W, Jiang J. Grain trajectory and grain workpiece contact analyses for modeling of grinding force and energy partition. Int J Adv Manuf Tech 2014;70:2111-2123.
[24] Johnson KL. Contact mechanics. Cambridge University press, 1987.
[25] Fischmeister HF, Arzt E. Densification of powders by particle deformation. Powder Metall 1983;26:82-88.
[26] Shaw MC. Principles of abrasive processing. New York: Oxford University Press; 1996.
[27] Park HW, Liang SY. Force modeling of micro-grinding incorporating crystallographic effects. Int J Mach Tool Manu 2008;48:1658-1667.
[28] Yuan ZJ, Zhou M, Dong S. Effect of diamond tool sharpness on minimum cutting thickness and cutting surface integrity in ultraprecision machining. J Mater Process Tech 1996;62:327-330.
[29] de Oliveira FB, Rodrigues AR, Coelho RT, de Souza AF. Size effect and minimum chip thickness in micromilling. Int J Mach Tool Manu 2015;89:39-54.
[30] Liu X, DeVor RE, Kapoor SG. An analytical model for the prediction of minimum chip thickness in micromachining. J Manuf Sci E-T ASME 2005;128:474-481.
[31] Malekian M, Mostofa MG, Park SS, Jun MBG. Modeling of minimum uncut chip thickness in micro machining of aluminum. J Mater Process Tech 2012;212:553-559.
[32] Ramos AC, Autenrieth H, Strauß T, Deuchert M, Hoffmeister J, Schulze V. Characterization of the transition from ploughing to cutting in micro machining and evaluation of the minimum thickness of cut. J Mater Process Tech 2012;212:594-600.
[33] Woon KS, Rahman M, Fang FZ, Neo KS, Liu K. Investigations of tool edge radius effect in micromachining: A FEM simulation approach. J Mater Process Tech 2008;195:204-211.
[34] S.M. Son, H.S. Lim, J.H. Ahn, Effects of the friction coefficient on the minimum cutting thickness in micro cutting. Int J Mach Tool Manu 2005; 45:529-535.
[35] Kim CJ, Mayor JR, Ni J. A static model of chip formation in microscale milling. J Manuf Sci E-T ASME 2005;126:710-718.